Intrazeolite Nanostructure of Nd(III) Complex Giving Strong Near-Infrared Luminescence

Munenori Ryo,[†] Yuji Wada,*[,†] Tatsuya Okubo,[‡] Yasuchika Hasegawa,[†] and Shozo Yanagida[†]

Material and Life Science, Graduate School of Engineering, Osaka University, Yamada-oka, Suita, Osaka, 565-0871, Japan, and PRESTO, JST and Department of Chemical System Engineering, The University of Tokyo, Bunkyo-ku, Tokyo, 113-8656, Japan

Received: April 14, 2003; In Final Form: August 20, 2003

We investigated the variation of the emission properties of tetramethylammonium ion-containing faujasite zeolite treated with bis-(perfluoromethylsulfonyl)amide (PMS) as a function of the Nd(III)-loading level. The emission intensity increased with the Nd(III)-loading level. The emission decays did not follow simple first-order kinetics and the average lifetime became longer with increasing Nd(III)-loading level. It was found that at low Nd(III)-loading levels, $Nd(PMS)_3$ complexes formed with coordinating water molecules in the supercage of the zeolite, resulting in rapid emission with a lifetime of less than 40 μs. On the other hand, the components with lifetimes longer than 100 μs observed at high loading levels were attributed to [Nd(PMS)]− zeolite complexes without coordinating water molecules. The zeolites with high Nd(III)-loading levels gave more efficient emission due to the large contribution of the complex in the zeolite that emitted more efficiently. The suppression of energy migration among the Nd(III) ions by co-exchanging with La(III) led to more efficient near-IR emission of Nd(III) complexes encaged in the faujasite-type zeolite.

Introduction

Nd(III)-containing systems have been regarded as the most popular infrared luminescent materials for application in laser systems. Developing a strongly luminescent Nd(III) center in organic media has been an attractive target because of its applicability to organic liquid lasers,[1] optical-fiber polymers,[2] organic electroluminescent devices,[3] and near-infrared immunoassays.[4] In general, effective luminescence of Nd(III) in organic media is achieved by excluding high vibrational bonds such as C−H and O−H from its surroundings[5−11] and distributing the ions homogeneously with distances long enough to suppress the cross relaxation process.[12] We successfully observed the Nd(III) luminescence in organic media using a complex with long perfluoroalkyl chains.[13,14] Recently, efficient luminescence of Nd(III) in organic media was achieved using dispersible inorganic $LaPO_4$ nanoparticles as a host matrix.[15]

Zeolites play indispensable roles in many technological and economical applications. Of primary importance are their uses as catalysts and molecular sieves. Zeolites have attracted scientists' interests as hosts of photochemically or optically active guests for constructing novel materials designed at nanosized levels.[16−18] Although luminescence of intrazeolite rare earth ions has been utilized mostly as an analytical tool for the topological assignment of ions to specific sites in these lattices,[19−24] their potential uses as new emitting materials have only been investigated recently.[25−34] Zeolites are attractive hosts for efficient near-IR luminescence of rare earth ions, because the zeolites consist of Si−O−Si and Si−O−Al frameworks having low vibrational frequencies, if water molecules and silanol groups in the pores are removed. Faujasite zeolites possess the ability to locate the ions separately as shown in Fujimoto's report,[35] in which the zeolite was used as a material separating Nd(III) ions with adequate distance in SiO_2 glass for the suppression of cross relaxation.

First attention was given to faujasite zeolite nanocrystallites[36,37] for applicability of strong emissive Nd(III) centers in organic media because of their dispersion stability. To obtain luminescence of Nd(III) in the cage of the zeolites, it is necessary to exclude coordinating water molecules and silanol groups from the vicinity of the ion. Calcination at high temperatures is undesirable especially for the nanocrystallites, because it induces their aggregation. We successfully enhanced the near-IR emission efficiency of Nd(III) in organic media by ligating it with bis-(perfluoromethylsulfonyl)aminate (PMS)[14] as a low vibrational ligand, in the cages of tetramethylammonium ion (TMA^+)-containing faujasite zeolite nanocrystallites.[38] We revealed therein that the presence of TMA^+ ions in the sodalite cages was important for strong emission.[39] Nd(III) cannot move to the inner cages such as the sodalite cage and hexagonal prism due to the steric hindrance by TMA^+ in the sodalite cage, and the ion is left in the supercage. Since the ligand PMS inducing luminescence of intrazeolite Nd(III) can penetrate only into the supercage, the Nd(III) left in the supercage is readily ligated by PMS.

In the present report, we have examined the dependence of the emission properties on Nd(III) concentration in the zeolite and discussed the intrazeolitic nanostructures of Nd(III) surroundings at each Nd(III)-loading level. Furthermore, on the basis of the obtained information, we have succeeded in enhancing the near-IR emission efficiency of the luminescent Nd(III) complex encapsulated in the zeolite by suppressing the energy migration between Nd(III) ions residing in the two different surroundings.

* Corresponding author. E-mail: ywada@mls.eng.osaka-u.ac.
[†] Osaka University.
[‡] The University of Tokyo.

10.1021/jp034993+ CCC: $25.00
Published on Web 09/20/2003

Experimental Section

Synthesis of the nanocrystalline zeolite was carried out according to a recipe reported in the literature[37] using a clear solution having a composition of 0.15 Na_2O:5.5 $(TMA)_2O$:2.3 Al_2O_3:10 SiO_2:570 H_2O. The procedure of the synthesis was as follows. Tetramethylammonium hydroxide solution (15 wt % TMAOH solution; Wako) was added to an aqueous solution of aluminum isopropoxide (Kishida) to give a clear solution. Then silica sol (30%, 5 nm, pH 10, Aldrich) was added while stirring, and the mixture was further stirred for 30 min. After 48 h of aging, the solution was heated at 373 K for 3 days. The resulting solid was separated by centrifugation (40 000 G) for 30 min, and washed with deionized water. The nanocrystallites were separated by centrifugation and dried at 358 K.

Zeolites with different Nd(III)-loading levels were prepared by adding the synthesized zeolite of 0.3 g to 30 mL aqueous solutions with different concentrations of $Nd(NO_3)_3 \cdot 6H_2O$ (0.001, 0.0025, 0.005, and 0.0075 M) at 353 K for 24 h. After the products were removed by centrifugation, they were washed with deionized water, and dried in air at 358 K. The amount of Nd(III) loaded into the zeolites was determined by ICP (JOBIN YVON, ULTIMA2). The ion exchange in 0.001, 0.0025, 0.005, and 0.0075 M solution yielded the zeolites containing 1.2, 4.4, 8.2, and 12.7 Nd(III) per unit cell, respectively. To prepare a fully Nd(III)-loaded zeolite, an ion exchange was carried out by stirring in 0.1 M aqueous solution of $Nd(NO_3)_3 \cdot 6H_2O$ at 373 K for 24 h. By this ion exchange, 14.3 Nd(III) per unit cell were introduced into the zeolite. Hereafter, we denote the zeolites with the different Nd(III)-loading levels as Nd1.3, Nd4.4, Nd8.2, Nd12.7, and Nd14.3 using the number of Nd(III) per unit cell. The zeolites loaded fully with Nd(III) and La(III) were prepared by stirring in 0.1 M aqueous solution of $Ln(NO_3)_3 \cdot 6H_2O$ (Ln = Nd, La) at 373 K for 24 h ([Nd(III)] = 0.01 M for Nd1.1La11.4, [Nd(III)] = 0.05 M for Nd6.0La7.7).

The Nd(III)-exchanged zeolites were degassed at 423 K for 30 min and exposed to vapor of PMS at 373 K for 1 h. The resulting samples were degassed at 423 K for 30 min, and then sealed under vacuum. A sequence of the operation was carried out in a vacuum line without exposing the zeolites to the atmosphere.

The amount of TMA^+ cation was estimated from the thermogravimetric (TG) profile and DSC curve (Shimadzu, TGA-50 and DSC-60). The amount of the adsorbed PMS was determined from the TG-DSC profiles. Emission spectra were obtained with a Fluorolog 3 (JOBIN YVON) equipped with a photomultiplier cooled at 193 K. Decay profiles monitored at 890 nm were recorded with a photomultiplier coupled to a Tektronix TDS3052 oscilloscope upon excitation with the second harmonic of a Nd:YAG laser (532 nm, >10 ns fwhp).

Results and Discussion

Structure of Nd(III) Complex in the Cage of the Zeolite. The DSC curves of the zeolites with different Nd(III)-loading levels are depicted in Figure 1. In the DSC curve of Nd(III)-unloaded zeolite, the peaks at 623 and 773 K were attributed to the decomposition of TMA^+ ions in the supercage and the sodalite cage, respectively, as reported by Saldarriaga et al.[40] The peak corresponding to the decomposition of TMA^+ in the supercage decreased as the amount of loaded Nd(III) increased. On the other hand, the peak due to the decomposition of TMA^+ in the sodalite cage was almost independent of the Nd(III) concentration. This indicates that the TMA^+ in the supercage was exchanged by Nd(III), although some TMA^+ ions in the sodalite cage resided without being exchanged by Nd(III). The

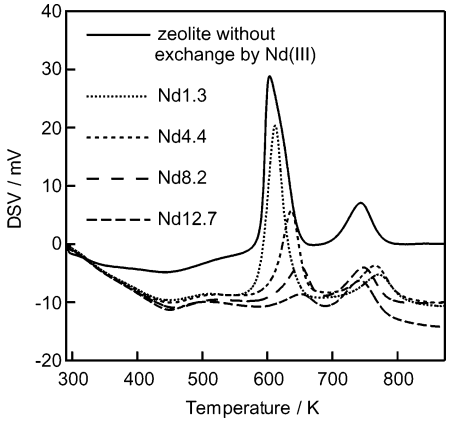

Figure 1. DSC curves of the zeolites with different Nd(III)-loading levels.

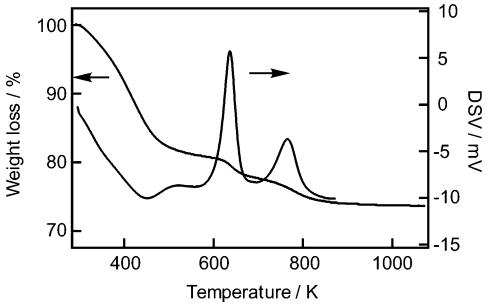

Figure 2. Examples of a thermogravimetric profile (left axis) and DSC curve (right axis) of the Nd(III)-exchanged zeolite (Nd4.4).

TABLE 1: Numbers of Each Cation Included in the Zeolites with Different Nd(III)-Loading Levels per Unit Cell Estimated by ICP and TG-DSC Measurements

			TMA	
sample	Nd	Na	supercage	sodalite cage
Nd1.3	1.3	32.8	12.2	8.4
Nd4.4	4.4	31.2	7.7	8.1
Nd8.2	8.2	19.0	5.4	7.8
Nd12.7	12.7	14.4	4.2	7.8
Nd14.3	14.3	10.5	3.1	8.3

numbers of TMA^+ in each cage were estimated from the weight loss in the TG profiles observed in Figure 2 for the case of Nd4.4. The obtained numbers of TMA^+ in each cage are listed in Table 1. Although the number of TMA^+ in the supercage decreased as the amount of loaded Nd(III) increased, the numbers of TMA^+ in the sodalite cages were approximately 8 in all the samples, corresponding to the number of sodalite cages per unit cell.

Although the decomposition of the $Nd(PMS)_3 \cdot 2H_2O$ complex at 623 K was confirmed by the DSC measurement, no clear peak due to the decomposition of the intrazeolite Nd(III) complex could be observed in the samples treated with PMS, because of an interference with TMA^+. It was reported that the desorption of water molecules in zeolites completed at 473 K and the decomposition of organics encapsulated into zeolites began at 573 K.[28,41,42] Hence, we tried to calculate the amount of PMS adsorbed into the pores of the zeolite from the difference between the weight of the zeolite treated with PMS and the untreated one at 573 K (for example, see Figure 3). The calculated amounts of PMS in the samples are listed in Table 2. The amount of PMS adsorbed into the zeolite tended to become small when the Nd(III)-loading level became large. Analogous tendencies were reported by Kynast and Taurines's papers, in which the amounts of the ligands such as 1-(2-

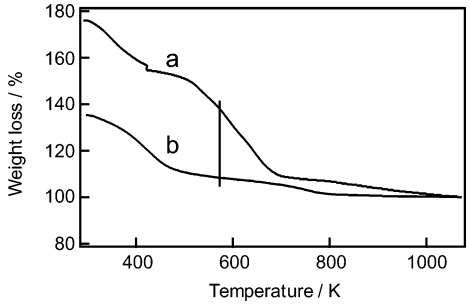

Figure 3. Thermogravimetric profiles of the Nd(III)-exchanged zeolite (Nd12.7) (a) with and (b) without treatment with PMS. The difference between the weights at 573 K of the zeolite with and without the treatment with PMS should correspond to the amount of PMS adsorbed into the zeolite.

TABLE 2: Numbers of Nd(III) Ions and PMS Molecules of the Nd(III)-Exchanged Zeolites Treated with PMS per Supercage

sample	Nd	PMS	PMS/Nd
Nd1.3	0.16	2.7	2.7
Nd4.4	0.55	1.9	1.9
Nd8.2	1	1.8	1.8
Nd12.7	1.6	1.8	1.1
Nd14.3	1.8	1.7	0.94

thenoyl)-3,3,3-trifluoracetate and the dipicolinate ion decreased when the Eu(III) content became large.[33,34] In the sample Nd1.3 with the lowest Nd(III)-loading level, the numbers of Nd(III) ions and the ligands PMS per supercage were 0.16 and 2.7, respectively. It is expected that the ion and the ligand distributed homogeneously in the supercage of the zeolite. Thus, 16 of 100 supercages should be occupied by one Nd(III), which is surrounded by 2.7 PMS molecules. This model led us to the conclusion that the $Nd(PMS)_3$ complex predominantly formed in one supercage. In the sample Nd14.3 with the highest Nd(III)-loading, which contained nearly two Nd(III) ions per a supercage, the ratio of PMS/Nd(III) in one supercage was 0.94. Hence, when two Nd(III) ions existed in one supercage, $[Nd(PMS)]^{2+}$ should form. The excess positive charge of $[Nd(PMS)]^{2+}$ would be balanced by the negative charge of the zeolite framework. So, we denote this complex as [Nd(PMS)]-zeolite, hereafter. The number of the supercages containing two Nd(III) ions should become large with the increase of the Nd(III)-loading level. The samples with more than 1 Nd(III) ion per supercage (Nd8.2, Nd12.7) must include the [Nd(PMS)]-zeolite complex.

Emission Properties of Nd(III)-Exchanged Zeolite Treated with PMS. Figure 4A shows the emission spectra of the samples treated with PMS. In all the samples, the characteristic sharp emission bands due to the $f-f$ transition were observed. The emission intensity increased as the Nd(III)-laoding level became large. The $^4F_{3/2}-^4I_{11/2}$ transition intensity was plotted as a function of the Nd(III)-loading level (Figure 4B). A parabolic increase of the emission intensity was observed with increasing Nd(III)-loading level.

Figure 5 shows the emission decay curves of the samples treated with PMS. In all the samples, the emission decays did not follow simple first-order kinetics. A reasonable fit of the decay curves was achieved by using a biexponential function except for the sample Nd8.2. The emission decay of Nd8.2 consisted of three components. The obtained emission lifetimes are listed in Table 3. The emission decays of all the samples contained a very short component with a lifetime of 5 μs. The components with the lifetime longer than 100 μs were observed in the samples with more than 8 Nd(III) per unit cell and

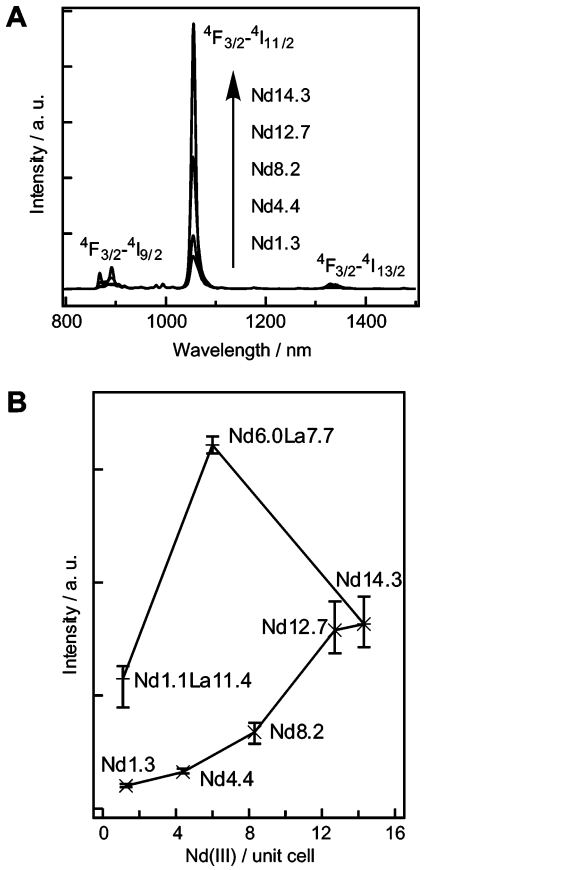

Figure 4. (A) Emission spectra of the PMS-treated zeolites with different Nd(III)-loading levels. The excitation wavelength was 580 nm. (B) Plot of $^4F_{3/2}$-$^4I_{11/2}$ transition intensity versus the number of Nd(III) per unit cell.

increased in the order of Nd8.2, Nd12.7, Nd14.3. The average lifetime tended to increase with the increase of the Nd(III)-loading level, being similar to the behavior of the emission intensity. It is concluded that in TMA^+-containing faujasite zeolite treated with PMS, the higher Nd(III)-loading level resulted in more efficient luminescence. The parabolic increase of the emission intensity is attributed to the synergistic effect of the increased absorption due to the higher Nd(III)-loading level and a corresponding enhancement of the emission efficiency.

Relationship between Intrazeolite Structure of Nd(III) Complex and Emission Property. In the sample Nd1.3 with the lowest Nd(III)-loading level, Nd(III) ions should exist as $Nd(PMS)_3$ in the supercage after the introduction of PMS. This complex has two coordinating water molecules when synthesized in water.[14] By TG-measurement, it was confirmed that the zeolite heated at 423 K before the PMS introduction contained a large amount of water molecules (50 per unit cell). Therefore, the $Nd(PMS)_3$ complex generated in the supercage should have coordinating water molecules. Taking into a consideration that the excited state of Nd(III) ion is quenched by O−H bond efficiently, it is derived that the shortest lifetime of Nd1.3 is caused by the coordinating water molecules.

The component with the lifetime longer than 100 μs appeared in the samples containing more than one Nd(III) ion per supercage (Nd8.2, Nd12.7, Nd14.3) and increased in the order of Nd8.2, Nd12.7, Nd14.3. This supports the view that the long component is attributable to the [Nd(PMS)]-zeolite complex, since the complex must be included to some extent in these samples. The increase of the average lifetime with the increase

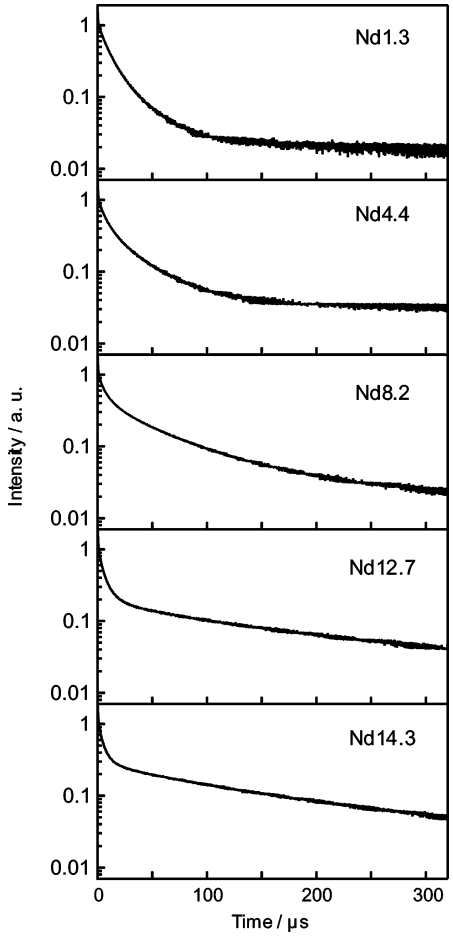

Figure 5. Emission decay curves monitored at 890 nm of the PMS-treated zeolites with different Nd(III)-loading levels upon excitation with the second harmonic of a Nd:YAG laser (532 nm).

TABLE 3: Emission Lifetimes of the Nd(III)-Exchanged Zeolites Treated with PMS

	τ/μs			τ_{avr}/μs
Nd1.3	7 (0.64)	26 (0.36)		14
Nd4.4	6 (0.59)	33 (0.41)		17
Nd8.2	5 (0.71)	35 (0.24)	148 (0.05)	19
Nd12.7	5 (0.80)		105 (0.20)	25
Nd14.3	4 (0.77)		110 (0.23)	28
Nd1.1La11.4	7 (0.64)		120 (0.36)	48
Nd6.0La7.7	6 (0.73)		145 (0.27)	37

of the Nd(III)-loading level is due to the high concentration of the [Nd(PMS)]-zeolite with a long emission lifetime.

In the sample Nd14.3, which included nearly two Nd(III) ions per supercage, two [Nd(PMS)]-zeolite complexes should generate in one supercage without the generation of $Nd(PMS)_3$ after the treatment by PMS. Two species of the [Nd(PMS)]-zeolite complex assuming different structures should exist, because of the emission decay with the components (4 and 110 μs). Since the excited state of Nd(III) ion is quenched by O−H bonds efficiently, the coordination of water molecules or silanol groups to the [Nd(PMS)]-zeolite complex thus causes the inefficient emission. On the other hand, the [Nd(PMS)]-zeolite complex with the longer component would not be coordinated by water molecules or silanol groups.

Optimizing the Emission Efficiency by Suppression of Excitation Migration on Nd(III). Cross relaxation and energy migration processes are nonradiative dipole−dipole energy transfers. According to Förester-Dexter theory, the rates of the nonradiative dipole−dipole energy transfer declines inversely with sixth power of the distance R between interacting centers. The rates of the processes ζ are calculated from the following equation:[43]

$$\zeta = A_r(R_{DA}{}^6/R^6) \quad (1)$$

where A_r is the total spontaneous emission rate and R_{DA} is the critical range at which the nonradiative energy transfer rate becomes equal to the spontaneous emission rate.

When two Nd(III) ions are included in one supercage, they assume a mutual distance of 8 Å, according to the geometrical calculation taking the coulomb repulsion into consideration. The critical ranges of the cross relaxation and the energy migration of Nd(III) in some glass matrixes were calculated to 3−4 and 9−11 Å, respectively.[35,43] The distance of 8 Å between the ions in the zeolite would allow the energy migration on Nd(III) ions but suppress the cross relaxation process. We have proposed that two species of the [Nd(PMS)]-zeolite with the fast and slow relaxation processes exist at high Nd(III)-loading level. The excitation migration would occur in the [Nd(PMS)]-zeolite with the slow relaxation more dominantly than in those with the fast relaxation. Once the excitation energy reaches [Nd(PMS)]-zeolite with the fast component, the excitation energy would be lost on the complex rather than migrating further. Hence, the suppression of the excitation migration should induce the more efficient luminescence of Nd(III) ions in the zeolite.

In general, the excitation migration can be suppressed by separating the ions by lowering the Nd(III)-loading level. However, in our zeolite system, Nd(III) ions locate in the lowest vibrational environment when fully loaded, as discussed above. By partially substituting Nd(III) with a different cation, dilution of Nd(III) should be achieved retaining the low vibrational surroundings of Nd(III). Since La(III) has the same radius as Nd(III) and does not participate in the energy migration, we prepared the zeolites loaded fully with Nd(III) and La(III) (sample Nd1.1La11.4 and Nd6.0La7.7). As shown in Figure 4B, the La(III)-substituted zeolites showed intense emission compared to the unsubstituted zeolites in the same magnitude of Nd(III) content after the treatment with PMS. The emission intensity reached a maximum at a number of 6 Nd(III) per unit cell. The emission intensity calibrated using the Nd(III) absorbance in each sample decreased with increasing Nd(III)-loading level as Nd1.1La11.4:Nd6.0La7.7:Nd14.3 = 9.1:4.7:1. This suggests that the emission is more efficient at lower Nd(III)-loading levels because of the more efficient suppression of the energy migration. More detailed information was obtained comparing the emission decay curves of the La(III)-substituted zeolites and Nd14.3 (see Figure 6). The lifetimes of the slower components of the La(III) co-exchanged zeolites were longer than that of Nd14.3, as shown in Table 3. When the excitation energy repeating the migration annihilates on the quenching site,

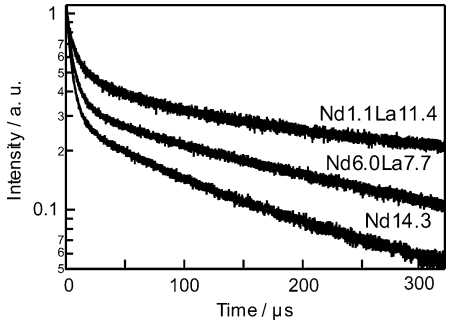

Figure 6. Comparison of the emission decay curves between the La(III)-substituted zeolites and unsubstituted zeolite.

the lifetime is shortened. Thus, the longer lifetimes of La(III)-substituted zeolites over non-La(III)-substituted zeolites is due to the suppression of excitation migration on Nd(III) ions with slow relaxation. The slow component increased as the Nd(III) content decreased. This result is thus interpreted as the suppression of excitation migration from the Nd(III) ions with the slow relaxation to the ones with fast relaxation occurring immediately after the first ion's absorption.

In the emission decay profiles of the dispersions of the zeolites exchanged with Nd(III) and co-exchanged with La(III) in deuterated dimethyl sulfoxide (DMSO-d_6), only slightly non-exponential behavior was observed in all the samples. By applying first-order kinetics, the same magnitude of lifetime was obtained in each sample (18 μs). These lifetime values were shorter than the average lifetimes in the powder samples. This is explained as follows: the organic molecules (DMSO-d_6) penetrate into the pores of the zeolite. Both the [Nd(PMS)]-zeolite complexes with the fast and slow relaxation processes assume equivalent environments with regard to DMSO coordination. As a result, their emission decays exponentially with identical components in all the samples. Hindering the penetration of the organic solvent molecules would thus lead more efficient luminescence of Nd(III) in the cage of the zeolites dispersed in organic media.

Conclusions

We investigated the dependence of the emission properties of TMA^+-containing faujasite zeolite treated with a low vibrational ligand on the Nd(III)-loading level. The emission intensity increased and the average lifetime became longer as the Nd(III)-loading level was increased. Inefficiency of luminescence at low Nd(III)-loading levels was caused by the $Nd(PMS)_3$ complexes having coordinating water molecules in the supercages of the zeolite. On the other hand, at high loading levels, the [Nd(PMS)]-zeolite complexes formed without coordinating water molecules in the supercages, resulting in more efficient emission. Furthermore, we succeeded in enhancing the near-IR emission efficiency of the complexes encaged in the zeolite by suppressing excitation migration by incorporating La(III) ions into the cage. In organic media, the luminescence efficiency of intrazeolite Nd(III) was reduced because of quenching by organic molecules which penetrated into the zeolite. Prevention of penetration of organic molecules, for example, by using a bulky ligand consisting of bonds with low vibrational frequencies, is expected to further improve the emission efficiency of zeolite-encaged Nd(III) dispersed in organic media.

Acknowledgment. This work was supported in part by Research for the Future Program, JSPS No. 12450345, and a Grant-in-Aid for Scientific Research on Priority Areas (417) from the Ministry of Education, Culture, Sports, Science and Technology (MEXT) of the Japanese Government (No. 15033245), and by the 21 COE Fellowship from Osaka University.

References and Notes

(1) Whittaker, B. *Nature* **1970**, *228*, 157.
(2) Kuriki, K.; Nishihara, S.; Nishizawa, Y.; Tagaya, A.; Koike, Y.; Okamoto, Y. *Electro. Lett.* **2001**, *37*, 415.
(3) Kawamura, Y.; Wada, Y.; Hasegawa, Y.; Iwamuro, M.; Kitamura, T.; Yanagida, S. *Appl. Phys. Lett.* **1999**, *74*, 3245.
(4) Werts, M. H. V.; Woudenberg, R. H.; Emmerink, P. G.; Gassel, R. V.; Hofstaat, J. W.; Verhoeven, J. W. *Angew. Chem., Int. Ed.* **2000**, *39*, 4542.
(5) Heller, A. *J. Am. Chem. Soc.* **1966**, *88*, 2058.
(6) Heller, A. *J. Am. Chem. Soc.* **1967**, *89*, 167.
(7) Haas, Y.; Stein, G.; Würzberg, E. *J. Chem. Phys.* **1974**, *60*, 258.
(8) Gösele, U.; Hauser, M.; Klein, U. K. A.; Frey, R. *Chem. Phys. Lett.* **1975**, *34*, 519.
(9) Gösele, U. *Chem. Phys. Lett.* **1976**, *43*, 61.
(10) Haas, Y.; Stein, G. J. *Phys. Chem.* **1971**, *75*, 3677.
(11) Beeby, A.; Faulkner, S. *Chem. Phys. Lett.* **1997**, *266*, 116.
(12) Burshtein, A. I. *Sov. Phys. JETP* **1983**, *57*, 1165.
(13) Yanagida, S.; Hasegawa, Y.; Murakoshi, K.; Wada, Y.; Nakashima, N.; Yamanaka, T. *Coord. Chem. Rev.* **1998**, *171*, 461.
(14) Hasegawa, Y.; Ohkubo, T.; Sogabe, K.; Kawamura, Y.; Wada, Y.; Nakashima, N.; Yanagida, S. *Angew. Chem., Int. Ed.* **2000**, *39*, 357.
(15) Hebbink, G. A.; Stouwdam, J. W.; Reinhoudt, D. N.; Veggel, F. C. J. M. V. *Adv. Mater.* **2002**, *14*, 1147.
(16) Maas, H.; Calzaferri, G. *Angew. Chem., Int. Ed.* **2002**, *41*, 2284.
(17) Ozin, G. A.; Kuperman, A.; Stein, A. *Adv. Mater.* **1989**, *3*, 69.
(18) Scaiano, J. C.; Garcia, H. *Acc. Chem. Res.* **1999**, *32*, 783.
(19) Arakawa, T.; Takakuwa, M.; Adachi, G.; Shiokawa, J. *Bull. Chem. Soc. Jpn.* **1984**, *57*, 1290.
(20) Benedict, B. L.; Ellis, A. B. *Tetrahedron* **1987**, *43*, 1625.
(21) Bartlett, J. R.; Cooney, R. P.; Kydd, R. A. *J. Catal.* **1988**, *114*, 58.
(22) Hazenkamp, M. F.; Veen, A. M. H. V. D.; Feiken, N.; Blasse, G. *J. Chem. Soc., Faraday. Trans.* **1992**, *88*, 141.
(23) Hong, S. B.; Shin, E. W.; Moon, S. H.; Pyun, C.-H.; Kim, C.-H.; Uh, Y. S. *J. Phys. Chem.* **1995**, *99*, 12278.
(24) Lee, S.; Hwang, H.; Kim, P.; Jang, D. *Catal. Lett.* **1999**, *57*, 221.
(25) Baker, M. D.; Olken, M. M.; Ozin, G. A. *J. Am. Chem. Soc.* **1988**, *110*, 5709.
(26) Kynast, U.; Weiler, V. *Adv. Mater.* **1994**, *6*, 937.
(27) Rosa, I. L. V.; Serra, O. A.; Nassar, E. J. *J. Lumin.* **1997**, *72*−*74*, 532.
(28) Alvaro, M.; Fornes, V.; Garcia, S.; Scaiano, J. C. *J. Phys. Chem. B* **1998**, *102*, 8744.
(29) Borgmann, C.; Sauer, J.; Jüstel, T.; Kynast, U.; Schüth, F. *Adv. Mater.* **1999**, *11*, 45.
(30) Chen, W.; Samynaiken, R.; Huang, Y. *J. Appl. Phys.* **2000**, *88*, 1424.
(31) Rocha, J.; Carlos, L. D.; Rainho, J. P.; Lin, Z.; Ferreira, P.; Almedia, R. M. *J. Mater. Chem.* **2000**, *10*, 1371.
(32) Jüstel, T.; Wiechert, D. U.; Lau, C.; Sendor, D.; Kynast, U. *Adv. Funct. Mater.* **2001**, *11*, 105.
(33) Sendor, D.; Kynast, U. *Adv. Mater.* **2002**, *14*, 1570.
(34) Dexpert-Ghys, J.; Picard, C.; Taurines, A. *J. Inclusion Phenom. Macrocyclic Chem.* **2001**, *39*, 261.
(35) Fujimoto, Y.; Nakatsuka, M. *J. Non-Cryst. Solids* **1997**, *215*, 182.
(36) Zhu, G.; Qui, S.; Yu, J.; Sakamoto, Y.; Xiao, F.; Xu, R.; Terasaki, O. *Chem. Mater.* **1998**, *10*, 1483.
(37) Mintova, S.; Olson, N. H.; Bein, T. *Angew. Chem., Int. Ed. Engl.* **1999**, *38*, 3201.
(38) Wada, Y.; Okubo, T.; Ryo, M.; Nakazawa, T.; Hasegawa, Y.; Yanagida, S. *J. Am. Chem. Soc.* **2000**, *122*, 8583.
(39) Ryo, M.; Wada, Y.; Okubo, T.; Nakazawa, T.; Hasegawa, Y.; Yanagida, S. *J. Mater. Chem.* **2002**, *12*, 1748.
(40) Saldarriaga, L. S. D.; Saldarriaga, C.; Davis, M. E. *J. Am. Chem. Soc.* **1987**, *109*.
(41) Casades, I.; Constantine, S.; Cardin, D.; Garcia, H.; Gilbert, A.; Marquez, F. *Tetrahedron* **2000**, *56*, 6951.
(42) Cano, M. L.; Cozens, F. L.; Fornés, V.; García, H.; Scaiano, J. C. *J. Phys. Chem.* **1996**, *100*, 18145.
(43) Caird, J. A.; Ramponi, A. J.; Staver, P. R. *J. Opt. Soc. Am. B* **1991**, *8*, 1391.